J Mater Sci: Mater Electron (2017) 28:16585–16597
DOI 10.1007/s10854-017-7612-0

REVIEW

A review of noble metal (Pd, Ag, Pt, Au)–zinc oxide nanocomposites: synthesis, structures and applications

Hang Liu[1,2,3] · Jiatai Feng[3] · Wanqi Jie[1,2]

Received: 29 March 2017 / Accepted: 28 July 2017 / Published online: 29 July 2017

Abstract As a promising candidate for future catalytic applications, the noble metal–ZnO nanocomposites are gaining increasing interest due its high catalytic property, and super stability. In this review, the noble metal–ZnO nanocomposites with various composites and structures for catalytic applications will be discussed. We introduce the multi-catalytic properties and design concept of the noble metal–ZnO nanocomposites, and then particular highlight key finding of synthesis method for various noble metal–ZnO nanocomposites. The catalytic activity of noble metal–ZnO nanostructures has been found to rely on not only the species of noble metal but also the architecture of the catalyst material. Moreover, the typical works of modification on noble metal–ZnO nanostructures have been introduced. Critically, the challenges for future research development and our future perspectives are presented.

1 Introduction

In recent years, there have been many kinds of nano-photocatalysts reported for their attractive applications, such as solar energy conversion [1], environmental purification [2], photoelectrical sensing [3], photoredox catalysis [4], and particularly using in photo-catalytic applications [5, 6]. Zinc oxide (ZnO), with its unique advantages including high electrical and environmental stability, high photoelectrical performance and low cost, is a typical photocatalyst in group II-VI and has been widely used in industrial fields [7–9]. The properties of ZnO materials largely rely on their structures, and thus many ZnO have been synthesized to particular shapes, like particles, rods, belts, tetrapods, spheres, flowers, needles, flowers and tubular whiskers [10, 11]. These ZnO nano-materials have good catalytic performance regarding their physio-chemical properties. However, the photocatalytic activity of ZnO nano-materials is not high enough for catalytic application, due to a high recombination rate of electron–hole pairs [12].

Using noble metal (Pd, Ag, Pt, Au)–ZnO nanocomposites is a strategy to enhance the nano-photocatalytic properties of ZnO materials [13–20]. The Pd-, Ag-, Pt- and Au–ZnO nanocomposites have reduced-rates of recombination of the electron–hole pairs, since there have been the metal-accumulated electrons and the photo-catalytic holes in these ZnO-based nanocomposites [21]. The enhanced properties of noble metal–ZnO nanocomposites indicate that they can be used as sensors, converters, energy generators and photocatalysts instead of ZnO materials. There has been also variety of structures of noble metal–ZnO nanocomposites reported, showing that noble metal–ZnO is able to be widely used in nanotechnology. The noble metal–ZnO nanocomposites can occur in zero- (0D) to three-dimensional (3D) structures, using different synthesis methods, where their structures can be sphere, rod, wire, sheet, belt-like, flower-like, pyramid-like, etc. These structures determine the properties and applications of noble metal–ZnO nanocomposites as catalysts. Thus, we feel that

✉ Hang Liu
liuhangnpw@gmail.com

[1] State Key Laboratory of Solidification Processing, Northwestern Polytechnical University, Xi'an 710072, China

[2] Key Laboratory of Radiation Detection Materials and Devices, Ministry of Industry and Information Technology, School of Materials Science and Engineering, Northwestern Polytechnical University, Xi'an 710072, Shaanxi, China

[3] Laboratoire de Chimie Physique Matière et Rayonnement, Sorbonne Universités, UPMC Univ Paris 06, 4 place Jussieu, 75252 Paris Cedex 05, France

it is essential to summarize key new developments in this emerging research frontier. Our aims are to provide the state-of-the-art of current research development, to point out key challenges faced by researchers, and to stimulate future research in creating noble metal–ZnO nanocomposites for wide practical application.

In this review, we first briefly introduce the various synthesis methods for the preparation of noble metal–ZnO nanocomposites. Subsequently summarize key finding of the influences including structure and composite of the noble metal–ZnO nanocomposites on the photo-catalytic properties. Furthermore, the catalytic application of the noble metal–ZnO nanocomposites is deeply discussed. Lastly, the challenges for future research development and our future perspectives are also presented.

2 Methods of synthesis

The typical works reporting nanostructures of noble metal–ZnO nanocomposites have been listed and discussed for their properties and catalytic applications in this review. These noble metal–ZnO nanocomposites, synthesized using different methods, were showed with different structures properties and applications in their reports. The synthesis methods include solution-based hydrothermal approaches, UV-irradiation, calcination, anneal, flame spray pyrolysis, sputtering, coating, etc. In a typical synthesis, one or more of these methods was employed.

2.1 Solution-based methods

The obtaining of noble metal–ZnO nanocomposites by the solution-based synthetic process is the subject of much interest, in view of the simplicity, low cost, reliability, repeatability and relatively mild conditions of synthesis, which are such as to deposition of noble metal on the ZnO surface with selected noble metal ions. A typical solution-based method was binding particles to the oxide support via amine route in solution, which was employed to synthesize Pd–ZnO nanocomposites [22]. The Ag–ZnO nanosheet was also achieved at room temperature by depositing Ag nanoparticles on the ZnO nanosheets in solution [23]. In another UV-assisted works, Pd–modified ZnO nanoparticles were fabricated by mixing $PdCl_2$ and ZnO in solution and then UV-irradiated for 6 h by a λ_{max}-365 nm mercury lamp [24].

2.2 High temperature-based methods

The high temperature-based method does not require the use of organic solvents or additional processing of the product, which makes it a simple and environmentally friendly technique. For example, similar to the UV-assisted approaches but with high temperature, a preparation of laser-induced Ag–ZnO nanoparticles was developed by Whang et al. [25], treating the Ag and ZnO precursors with laser beam of 10 Hz for 30 min and annealing at 500 °C for 2 h. There have been many works reported using calcination techniques. The Pd–ZnO nanoparticles was achieved by mixing $PdCl_2$ in ZnO-nanoparticles-contained solution along with a calcination process at 250 °C [26]. The synthesis method of Au@ZnO core–shell nanoparticles was developed by heating Au nanoseeds and ZnO precursors together at 500 °C in air for 2 h [27]. More reported works of Pt–ZnO nanoparticles fabricated by solution-based mixing and annealing/calcining were also available [28, 29].

Some Pd–ZnO nanoparticles were synthesized by flame spray pyrolysis. Typically, the flame spray pyrolysis evaporated and combusted the ZnO and Pd precursor's droplets (in toluene/acetonitrile mixture solution), leading to a Pd deposition on ZnO powder support [30]. The synthesis of Au- and Pt–ZnO nanoparticles using a spray flame reactor was described in a report work [31] as well, using similar operating conditions as that of the Pd–ZnO synthesis. There has been a work using Au as core but decoration to synthesis the ZnO nanoflowers [32]. The Au–ZnO nanoflowers were fabricated by mixing ZnO and Au precursors in organic solution and heating at 120 °C for 15 min and 260 °C for 1 h. The noble metal–ZnO nanocomposites was attained by this synthetic method consumed much energy for the high temperature.

2.3 Electrical methods

Electro-synthesis method is the synthesis of chemical compounds in an electrochemical cell. The main advantage of electro-synthesis over an ordinary redox reaction is avoidance of the potential wasteful other half-reaction and the ability to precisely tune the required potential. With electrical methods, electrodeposition of Pt on ZnO nanorods was performed using an electrochemical analytical instrument prior to a 10 h-long annealing process (200 °C in air) [33], Coating of sputtered Pt on ZnO nanoparticles was another method to produce Pt–ZnO nanoparticles, reported by Phan and Chuang [34]. Pd-doped ZnO nanofibers were fabricated by electrospinning-assisted mixing and calcining at 600 °C in air for 3 h [35].

Based on the core–shell approach, the synthesis of ZnO@Pt nanoflowers was developed for ethyl violet decomposition by Yuan et al. [36], by heating the solution containing Pt seeds and ZnO precursors at 280 °C (Table 1).

Table 1 The material structures, synthesis methods, properties and applications of typical noble metal–ZnO nanocomposites

Material structure	Synthesis method	Properties/Applications	Reference
Pd–ZnO nanoparticles	Mixing in solution and UV-irradiated	Increased surface content of adsorbed oxygen; enhanced ability of photocatalytic oxidation of organics	[24, 37]
Pd–ZnO nanoparticles	Mixing in water and calcining at 250 °C	Highly crystalline; enhanced ability for sensing LPG and EtOH	[26]
Pd nanoparticles on ZnO powder support	Binding particles to the oxide support via amine route in solution	High conversion of CO to CO_2	[22]
Pd–ZnO nanoparticles	Flame spray pyrolysis	High sensitivity and fast response times for ethanol sensing	[30]
Pd-nanoparticles-decorated ZnO nanowires	Mixing the pre-synthesized Pd-nanoparticles and ZnO nanowires and then calcining at 600 °C	Enhanced response to H_2S gas	[38]
Pd-nanoparticles-decorated ZnO nanowires	Spin-coating Pd-nanoparticles on ZnO nanowires at 1000 rpm and calcining at 500 °C	Higher and faster photosensitivity; band-edge emission decreases and defect emission increases	[39]
Pd-nanoparticles-decorated ZnO nanorods	Mixing raw ZnO nanorods with $PdCl_2$ in ethanol solution under a 365 nm-UV light at room temperature	Enhanced CO sensing	[40]
Pd-doped ZnO nanofibers	Electrospinning and calcining at 600 °C in air for 3 h	Enhanced CO sensing	[35]
Pd-nanoparticles-decorated ZnO nanosheets	Mixing Pd nanoparticles with ZnO nanosheets in water and annealing at 600 °C for 2 h	High selectivity and response speed for acetone sensing	[41]
Pd- and Au-nanoparticles-decorated ZnO nanobelts	Combining Pd or Au films with ZnO supports and annealing the mixture at 300 °C for half an hour in vacuum	Increased intensity of visible-light emission and decreased intensity of UV emission; enhanced sensitivity of acetone sensing	[42]
Pd–ZnO nanoflowers	Mixing ZnO and Pd precursors in aqueous solution and heating at 180 °C for 2 h in autoclave	High sensitivity in gas detection of ethanol	[43]
Pd-, Ag- and Pt-deposited sponge-like ZnO microcuboids	Mixing the noble metal precursors with ZnO microcuboids in aqueous solution and UV- irradiating for 4 h	High photo-generation rates of electron–hole pairs; high decomposition ability of acid orange II	[44]
Ag–ZnO nanoparticles	Treating the Ag and ZnO precursors with laser beam of 10 Hz for 30 min and annealing at 500 °C for 2 h	Improved visible-light sensitivity and phtocatalytic acitivity for degrading methylene blue	[25]
Ag–ZnO nanoparticles	Heating Au nanoseeds and ZnO precursors together at 500 °C in air for 2 h	High selectivity and sensitivity to hydrogen gas	[27]
Ag–ZnO nanowires	Electrospinning and calcining at 500 °C in air for 1 h in air	Enhanced photo-induced electron-transfer reactions	[45]
Ag–ZnO nanosheets	Depositing Ag nanoparticles on the ZnO nanosheets in solution	Improved photocatalytic activity with evaluated separation rate of electron–hole pairs	[23]
Ag- and Au–ZnO nanoflowers	Fabricate the flower-like ZnO nanostructure; load the Ag or Au nanoparticles on ZnO by a UV-irradiation of 15 min	High photocatalytic activity for degrading methylene blue	[46]
Ag–ZnO nanoflowers	Mixing ZnO and Ag precursors in aqueous solution and heating at 180 °C for 24 h in autoclave	440 nm-peak appeared on the UV–Vis absorption spectra	[47]
Ag–ZnO hollow microspheres	Mixing ZnO and Ag precursors and heating at 120 °C for 8 h	Increased charge separation and surface hydroxyl content number; high photocatalytic activity for degrading orange G	[48]
Pt–ZnO nanoparticles	Using solution-based Pt-film-coating and annealing of 600 °C for 30 min	Enhanced hydrogen sensing	[28]
Pt–ZnO nanoparticles	Calcining the Pt–ZnO mixture at 550 °C for 2 h	Phenol degradation	[29]

Table 1 (continued)

Material structure	Synthesis method	Properties/Applications	Reference
Pt–ZnO nanoparticles	Coating of sputtered Pt on ZnO nanoparticles	High sensitivity for H_2 detection	[34]
Pt–ZnO nanorods	Using electrodeposition and annealing at for 10 h 200 °C in air	Photoelectrochemical water splitting	[33]
Pt–ZnO nanoflowers	Mixing ZnO and Pt precursors in aqueous solution and heating at 180 °C for 2 h in autoclave	Enhanced optical and sensing properties for ethanol gas	[49]
Pt–ZnO nanoflowers	Heating the solution containing Pt seeds and ZnO precursors at 280 °C	Enhanced photocatalysis for ethyl violet decomposition	[36]
Au–ZnO nanoparticles	Mixing ZnO and Au precursors calcining at 550 °C	Visible light photocatalytic hydrogen production and degradation dye activities	[50]
Au–ZnO nanosheets	Loading Au on ZnO materials and then annealing at 600 °C for 1 h in O_2	Higher NO sensitivity rather than CO and other volatile organic compounds	[51]
Au–ZnO nanoflowers, nanomultipods and nanopyramids	Mixing ZnO and Au precursors in organic solution and heating the mixtures	High photocatalytic activity for decomposing rhodamine B	[32]
Au–ZnO nanopyramids	Regulating the heterogeneous nucleation and selective growth of ZnO on pre-synthesized Au seeds	High photocatalytic efficiency for decomposing rhodamine B	[52]
Au–ZnO nanoflowers	Mixing ZnO and Au precursors in aqueous solution and heating at 120 °C for 1 h in autoclave	Improved sensor response, selectivity; short response and recovery times to acetone vapor	[53]
Au–ZnO with comet-like structure	Mixing ZnO and Au precursors and heating at 160 °C for 24 h in autoclave	Surface plasmon resonance of the Au particles	[54]
Au–ZnO with mandarin orange-like structure	Mixing ZnO and Au precursors and heating at 160 °C for 24 h in autoclave	Changed optical absorption properties	[55]
Mg^{2+} doped Pd–ZnO nanostructure	Mixing molecules in solution and calcining them at high temperature for hours	Enhanced oxidative coupling of carbon monoxide to dimethyl oxalate	[56]
Graphene-Pd/Ag/Pt/Au–ZnO nanostructures	Mixing graphene with ZnO nanorods in solution and heating the sample in autoclave at 180 °C for 3 h to produce graphene–ZnO nanocomposites; loading Pd, Ag, Pt or Au nanoparticles on the graphene–ZnO nanocomposites with UV-irradiation for 30 min	High electrocatalysis for H_2O_2 reduction	[8]
Graphene-Pt/Pd–ZnO nanocomposites	Mixing and annealing	High methanol oxidation under visible-light exciting	[57]

3 Photocatalytic property

3.1 Structures (0–3D)

Since the majority of catalytic reactions are structure-sensitive or site-demanding, it is imperative to fundamentally understand the relationship between the structure or shape of nanomaterials and their electrocatalytic properties. However, in contrast to the growing number of studies on the correlation between the size of spherical nanoparticles and their catalytic activity, very little theoretical work has been conducted to evaluate the effects of nanoparticle shape on photo-catalytic activity of noble metal–ZnO nanocomposites since these structures are not easily accessible. Morphology control plays a key role in developing high-performance catalysts with unique physical and chemical properties as reported in the literature. Thus, the structures from zero dimension to three dimension of noble metal–ZnO nanocomposites will be discussed below. A nanoparticle structure is generally regarded as zero-dimensional (0D). Based on the nanosized structures, Fig. 1a shows a schematic diagram of photo-involved catalysis on a semiconductor, where the photocatalyst provides reactants the required reaction energy by converting the energy from light. The excited electrons can jump to conduction bands from valence bands with a generation of h^+ holes in the valence bands, when the photocatalyst is exposed to a light with energy not lower to the energy bandgap. Then the reactants on or near the surface of photocatalyst can use the band gap energy to initiate the reaction. A typical structure of Pd–ZnO nanocomposites is sphere particle, which can be achieved using solution-based approaches. A newly developed method is fabrication of Au–ZnO nanoparticles from zeolitic imidazolate framework-8 (ZIF8), for improved photocatalytic activities. Since the structure of Pd–ZnO nanocomposites plays an important role in their properties and applications, many works have been carried out to explore novel structures of Pd–ZnO nanocomposites based on previous studies of Pd–ZnO nanoparticles. As shown in Fig. 1b, ZnO supports with certain structures provide space for noble metals nanoparticles to attach, forming noble metal–ZnO interfaces of a Schottky contact. The noble metal–ZnO interfaces also can wide the nearby depletion-layer for a better electrons transporting among ZnO and Pd molecules [43]. Since the structure of Pd–ZnO nanocomposites plays an important role in their properties and applications, many works have been carried out to explore novel structures of Pd–ZnO nanocomposites based on previous studies of Pd–ZnO nanoparticles. A recent reported Au–ZnO nanocomposite [50], prepared from ZIF8by a mixing-calcination method (Fig. 2a), was observed under TEM with notable morphology differences for ZnO (Fig. 2b) and Au–ZnO nanoparticles (Fig. 2c).

Wire, rod and fiber are typical one-dimensional (1D) structures. typical Pd-nanoparticles-decorated ZnO nanowires (Fig. 3) were fabricated by Li's group [38]. The TEM images showed a clear structure of ZnO nanowires with the Pd-nanoparticle decoration, indicating good electrons transportability from ZnO to Pd molecules. A similar Pd–ZnO nanostructure (Pd nanoparticles on ZnO nanowires) was achieved by Bera and Basak [39]. The Pd-decorated ZnO nanowires showed a higher UV photosensitivity and response speed compared to the pure ZnO nanowires. Due to the enhanced energy transfer among ZnO and Pd molecules, when the Pd density increased, the photoluminescence spectrum of their Pd–ZnO nanowires showed a decreased band-edge emission and an increased defect-related emission. Through a similar approach, the Ag–ZnO nanowires were synthesized. The Ag-modification enhanced the photo-induced electron-transfer reactions of ZnO [45].

High ratio of surface area to volume is an important characteristic for effective interactions between materials and chemicals [58, 59]. The fabrication of ZnO-based photocatalysts has been desired with a high ratio of surface area to volume, like 2D platelike ZnO, leading to an improved activity than rodlike structures [60]. Porous ZnO nanosheets, produced by Xiao et al. [41], were used as

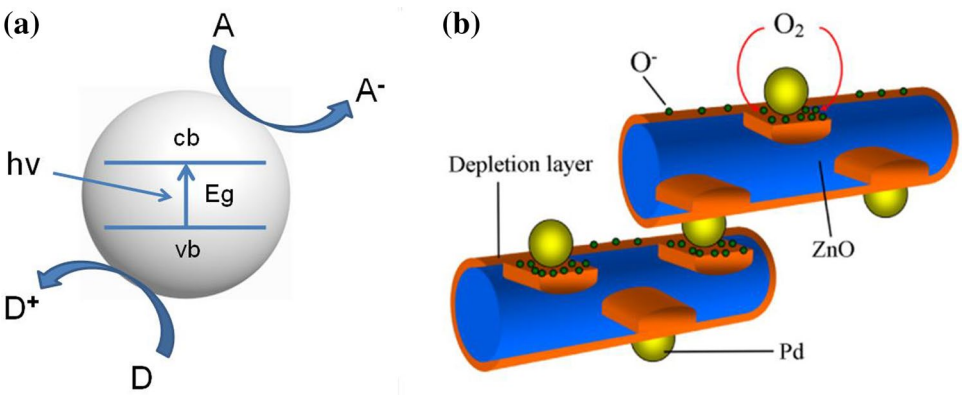

Fig. 1 Schematic diagrams of photo-involved catalysis on a semiconductor (**a**) and noble metal-decorated ZnO nanostructures (**b**) [43]

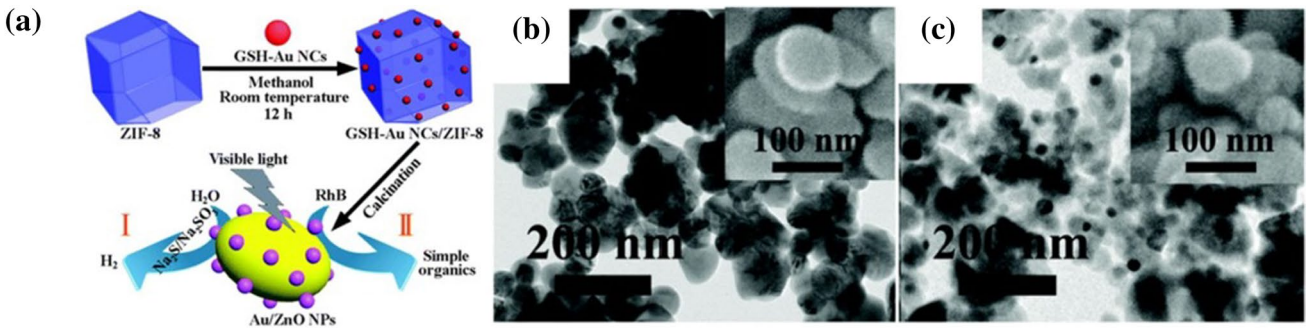

Fig. 2 Schematic diagrams of fabrication of Au–ZnO nanoparticles from ZIF8 (**a**), and the TEM images of ZnO (**b**) and Au–ZnO (**c**) nanoparticles [50]

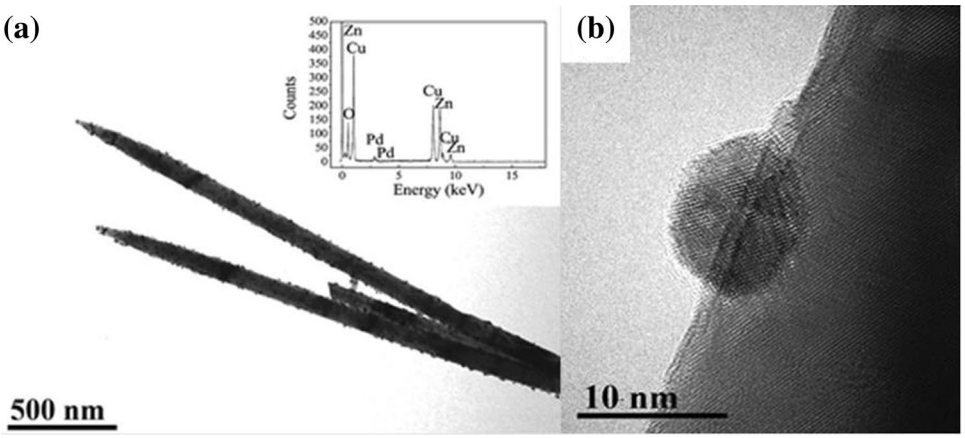

Fig. 3 The Pd-nanoparticles-decorated ZnO nanowires with elemental identification (**a**) and the magnified TEM image (**b**) [38]

support to load Pd nanoparticles by mixing the Pd nanoparticles with the ZnO nanosheets in water (self-assembling) and then annealing the mixture. Another 2D nanostructure of noble metal-nanoparticles-decorated ZnO was reported with a belt-like shape, synthesized by combining Pd or Au films with ZnO supports [42]. The decoration of noble metal on ZnO nanobelts increased the intensity of their visible-light emission but decreased the intensity of their UV emission. The fabricated Ag–ZnO nanosheets showed improved photocatalytic activity with evaluated separation rate of electron–hole pairs [23].

A novel 3D-structure is nanoflower, namely flower-like nanostructure. The formation of nanoflower or flower-like structure is generally accompanied with processes including crystallization, growth (molecular binding), self-assembling, micro-twisting, Ostwald ripening, etc [61–63]. Similar to some approaches of 1D/2D-nanostructure synthesis, flower-like Ag–ZnO and Au–ZnO nanostructures were fabricated using a two-step method: fabricate the flower-like ZnO nanostructure; load the Ag or Au nanoparticles on ZnO by a UV-irradiation of 15 min [46]. However, the noble metals were hard to be loaded uniformly on the ZnO supports via the two-step approach, may limiting their physio-chemical properties in some applications. To overcome this problem, some works have been carried out to fabricate 3D structures with nanoflower or flower-like nanostructure by one-step synthesis. Xing et al. [43] synthesized the Pd–ZnO nanoflowers (Fig. 4a) via hydrothermal route, mixing ZnO and Pd precursors in aqueous solution and heating at 180 °C for 2 h in autoclave. Similarly, Ag–ZnO nanoflowers (Fig. 4b) were prepared by mixing ZnO and Ag precursors in aqueous solution and heating at 180 °C for 24 h in autoclave, generating a 440 nm-peak appeared on the UV–Vis absorption spectra [47]. Pt–ZnO nanoflowers (Fig. 4c), with enhanced optical properties, were fabricated by mixing ZnO and Pt precursors in aqueous solution and heating at 180 °C for 2 h in autoclave [49]. Au-nanoparticles-decorated ZnO nanoflowers (Fig. 4d) were achieved by mixing ZnO and Au precursors in aqueous solution and heating at 120 °C for 1 h in autoclave [53]. Unlike above flower-like nanostructures, there has been a work using Au as core but decoration to synthesis the ZnO nanoflowers [32]. TEM images showed that the urchin-like (Fig. 4e) and petal-like (Fig. 4f) ZnO of Au–ZnO nanoflowers were located on

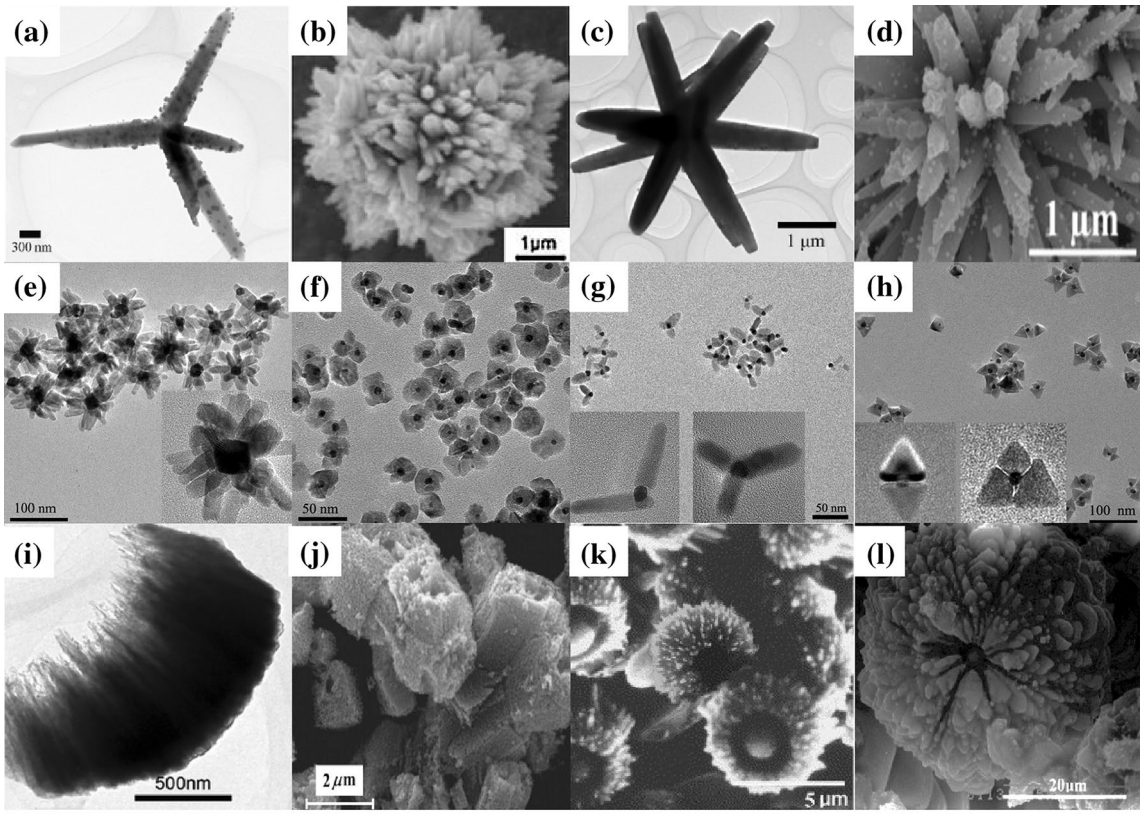

Fig. 4 3D structures: ZnO nanoflowers decorated with Pd (**a**) [43], Ag (**b**) [47], Pt (**c**) [49] and Au (**d**) [53]; urchin-like (**e**) and petal-like (**f**) Au–ZnO nanoflowers, Au–ZnO nanomultipods (**g**) and nanopyramids (**h**) [32]; Ag–ZnO hollow microspheres (**i**) [48]; sponge-like ZnO microcuboids (**j**) [44]; Comet-like (**k**) [54] and mandarin orange-like (**l**) [55] Au–ZnO structure

the Au cores. In the evaluation test of catalytic activity, the urchin-like Au–ZnO nanoflowers behaved better than the petal-like ones. They also fabricated multipod-like (Fig. 4g) and pyramid-like (Fig. 4h) Au–ZnO nanostructures using a similar method. The Au–ZnO nanomultipods showed a higher and the Au–ZnO nanopyramids showed the highest photocatalytic activity compared to the Au–ZnO nanoflowers for the following reason. There was a decreasing order of crystallinity: nanopyramids > nanomultipods > urchin-like nanoflowers > petal-like nanoflowers. Thus the well-crystallized Au–ZnO nanostructures had higher charge transfer activity and thus better photocatalytic efficiencies.

Another 3D nanostructure was created by Lu et al. [48] that the ZnO and Ag precursors were mixed and heated at 120 °C for 8 h in autoclave to produce Ag–ZnO hollow microspheres (Fig. 4i). The Ag deposits on ZnO increased the charge separation of hole-electron pairs and the number of surface hydroxyl content, resulting in a higher photocatalytic activity for degrading orange G. Noble metals-deposited sponge-like ZnO microcuboids (Fig. 4j) were fabricated by mixing the noble metal precursors with ZnO microcuboids in aqueous solution and UV-irradiating (365 nm) for 4 h [44]. Moreover, some other 3D structures were reported with shapes of comet-like (Fig. 4k) [54], mandarin orange-like (Fig. 4l) [55], etc.

3.2 Composite

To date, many noble metal–ZnO nanocomposites catalysts (M/ZnO, M = Au, Pt, Ag, Pd) have been successfully synthesized. The property of a nanoparticle material mainly relies on its composites. The Pd incorporation in ZnO can largely enhance the activity of ZnO nanoparticles for photocatalytic activity by decreasing the recombination rate of electron–hole pairs [64]. However, the effect of Pd modification was higher than that of Ag modification in their work, which might be explained by the increased charge separation rate and the increased surface hydroxyl content [37]. The difference of Au- and Pt–ZnO nanoparticles was described in a report work [31]. Although they found that the TEM images of Au–ZnO nanoparticles and Pt–ZnO nanoparticles were similar, the results showed that only the Au–ZnO nanoparticles had enhanced photocatalytic activity than raw ZnO nanoparticles, but the Pt–ZnO nanoparticles, for the following reason. The contact between Pt and

ZnO was ohmic, which may result in a discharge of electrons to electrolytes. The UV-irradiation method for ZnO nanorods preparation was further explored by Chiou et al. [21], using Au and Ag precursors for ZnO modification. The sputtered-Pt-coated ZnO nanorods were used to compare in this work as well. The energy of bandgaps using XES (X-ray emission spectroscopy) and XANES (X-ray absorption near edge structure) spectra were measured for these noble metal–ZnO nanorods, showing the order: Au (3.3 eV) < Pt (3.5 eV) < Ag (3.6 eV) (Fig. 5a). However, the methyl orange photodegradation tests (Fig. 5b) showed that only the Au- and Ag–ZnO nanorods with low density of noble metals and longer synthesis time had higher photocatalytic activity than raw ZnO nanorods. Thus, the photocatalytic acitivity of noble metal–ZnO nanostructures can be determined not only by the species of noble metals, but also the operating conditions of synthesis. Pd or Au films with ZnO supports and subsequently annealing the mixture at 300 °C for half an hour in vacuum [42]. The decoration of noble metal on ZnO nanobelts increased the intensity of their visible-light emission but decreased the intensity of their UV emission, and the decoration also enhanced the sensitivity for acetone sensing. However, in their work, the Pd–ZnO nanostructure showed a higher sensitivity than the Au–ZnO nanostructure may for the following reason. The Pd–ZnO is less defective regarding oxygen vacancy content than the Au–ZnO, resulting in more adsorption of O_2, since a sensing ability is related to the oxygen vacancy content [65]. For flower-like ZnO nanostructures, the noble metal-decorations enhance the photo-generation rates of electron–hole pairs, resulting in a higher photocatalysis. A typical work showed that the Ag-decoration flower-like ZnO nanostructure had a better degradation-photocatalysis than the Au-decoration flower-like ZnO nanostructure [46]. The photocatalytic ability of Ag, Pd and Pt decoration was also reported in another work with the order of Pd > Ag > Pt [44], regarding the production of ·OH radicals for dye decomposition [66]. However, Although the elemental activity of Pd, Ag, Pt and Au has the constant order, it is controversial that there is a constant order of catalytic activity for these noble metal–ZnO nanostructures. The catalytic activity of noble metal–ZnO nanostructures has been found to rely on not only the species of noble metal but also the operating conditions of synthesis, nanoparticle size of noble metal, distribution of nanoparticles, nanostructures and so forth.

XRD spectra show evidence of the successful synthesis and the crystal structures of metal–ZnO nanostructures. All XRD diffraction peaks of the noble metal–ZnO nanostructures can be indexed as a combination of the crystalline structure of noble metal and ZnO. As shown in Fig. 6a [67], the XRD spectra of tube-like, flower-like, star-like and skin needling-like Pd/ZnO composites are indexed as a combination of the face-centred-cubic structure of Pd and the wurtzite structure of ZnO. As shown in Fig. 6b [63], typical XRD 2θ peaks of ZnO sample are at 32°, 34°, 36°,

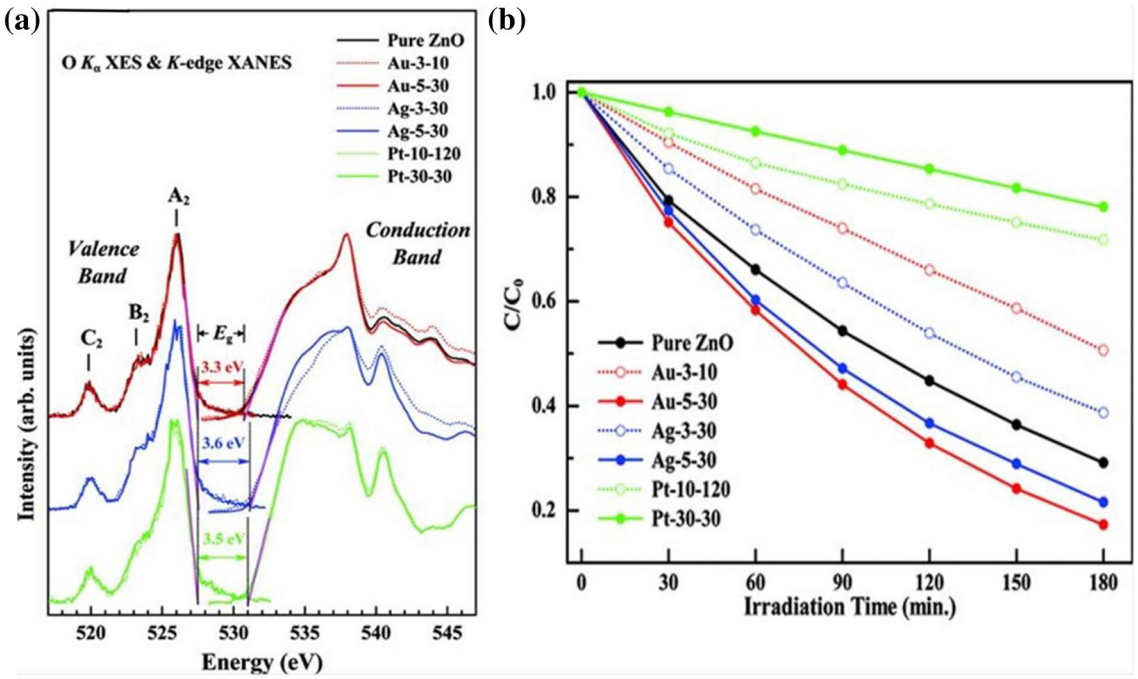

Fig. 5 The energy bandgap measurement using XES and XANES spectra for raw, Au-, Ag- and Pt–ZnO nanorods (**a**); the methyl orange photodegradation of raw, Au-, Ag- and Pt–ZnO nanorods (**b**) [21]

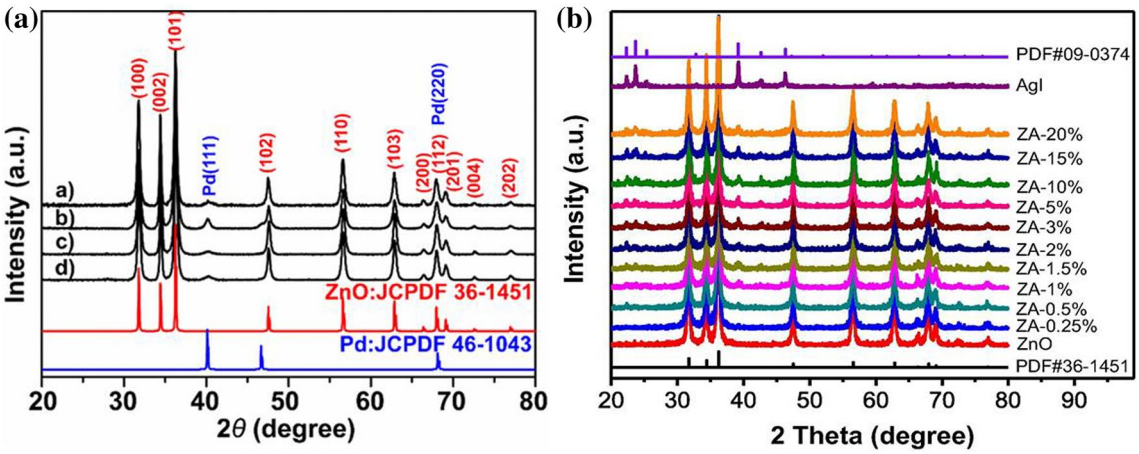

Fig. 6 XRD spectra of the tube-like, flower-like, star-like and skin needling-like Pd/ZnO composites [67] (**a**). XRD spectra of the synthesized ZnO-AgI composites [63] (**b**)

48°, 57°, 63°, 66°, 32°, 68° and 69°, showing the wurtzite crystal planes of ZnO including (100), (002), (101), (102), (110), (103), (200), (112) and (201). XRD spectra of the synthesized ZnO–AgI composites can be indexed as a combination of the crystalline structure of AgI and the wurtzite structure of ZnO. The XRD spectra are used to reveal the crystal structures of the noble metal–ZnO composites.

4 Application

4.1 Sensor

The fabricated noble metal–ZnO materials showed high selectivity and sensitivity to hydrogen gas [27]. Typically, the Pd–ZnO nanocomposites had a low operating temperature and an improved sensing ability for LPG- and EtOH-sensing [26]. The Pt–ZnO nanoparticles was used for hydrogen sensing in some other works [28, 34]. The Pd-nanoparticles-decorated ZnO nanowires fabricated by Li's group [38] presented an improved ability for sensing H_2S, compared to bare ZnO nanowires. The 2D Pd–ZnO nanoarchitectures, consisting of Pd nanoparticles and ZnO nanosheets, showed high selectivity and response speed for acetone sensing [41]. With particular properties, a typical 2D Au–ZnO nanosheet was found to have higher NO sensitivity rather than CO and other volatile organic compounds [51]. The Au–ZnO nanosheets were prepared by loading Au on ZnO materials and then annealing at 600 °C for 1 h in O_2 (Fig. 7a). After the photoreduction synthesis, the white solution containing ZnO and Au became deep red color, described by the authors. Their TEM image (Fig. 7b) clearly showed that the Au nanoparticles were decorated on the ZnO nanosheets. As a 2D structure, the Au–ZnO nanosheets had large surface-to-volume ration, resulting in more O_2 adsorbed on the nanostructures. Thus the broad surface depletion layer of Au–ZnO nanosheets provided a fast electrons transporting for ZnO, Au and surrounding NO molecules (Fig. 7c). Besides, the flower-like Pd–ZnO nanocomposites (Fig. 7a) showed a promising sensitivity in gas detection of ethanol, CH_4, CO and H_2 [43].

4.2 Waste degradation in environmental engineering

Since the O_2 composition and charge transfer on the surface points of a photocatalyst particle are related to the photocatalytic activity [68], Jing et al. measured these parameters by XPS (X-ray photoelectron spectroscopy) and SPS (Surface photovoltage spectroscopy) for Pd- and Ag–ZnO nanoparticles, which were synthesized by UV irradiation of the Pd–ZnO mixture solution [37]. Their phenol degradation tests indicated that the noble metal-modification largely increased the photocatalysis of ZnO, with enhanced O_2 composition and charge transfer. The Pd–ZnO nanocomposite had an increased surface content of adsorbed oxygen and thus an enhanced ability of photocatalytic oxidation of n-C_7H_{16} [24]. The Ag–ZnO nanoparticles showed largely improved visible-light sensitivity and photocatalytic acitivity for degrading methylene blue [25]. The reported works of Pt–ZnO nanoparticles fabricated by solution-based mixing and annealing/calcining were also available, for catalytic applications and phenol degradation [29]. These flower-like ZnO nanostructures had a higher photocatalytic activity than ZnO microrods in degrading methylene blue, and the noble metal-decoration further enhanced the photocatalysis [46]. For a high catalytic activity of decomposing rhodamine B, the Au–ZnO nanopyramids were prepared in another work by depositing ZnO molecules on Au nanocrystals at increased temperature for a few minutes [52]. Based on a similar core–shell approach, the synthesis

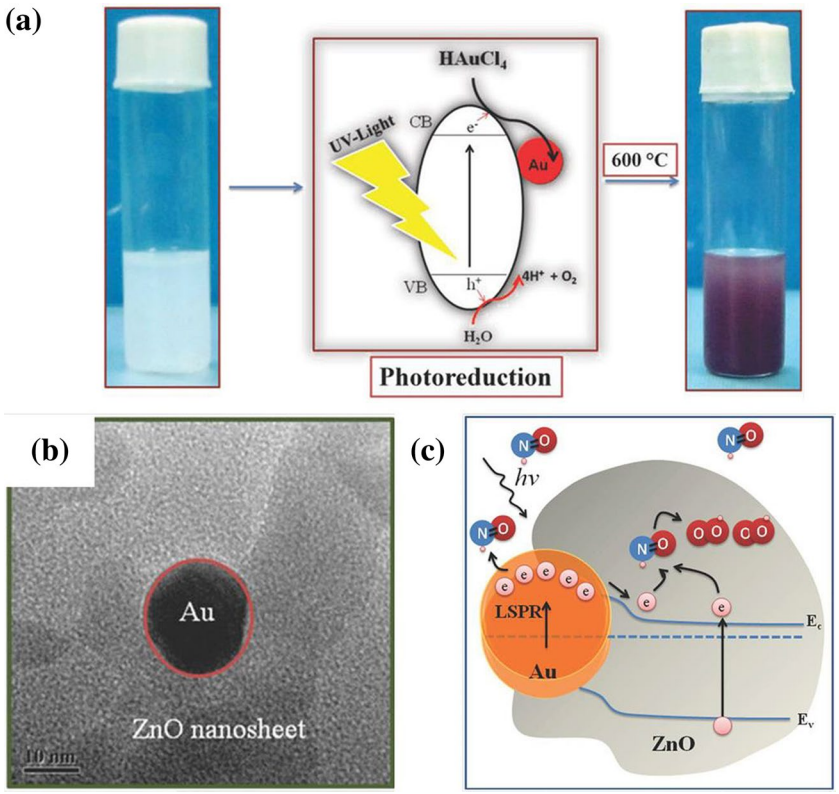

Fig. 7 The synthesis process of Au–ZnO nanosheets (**a**), TEM image of the Au–ZnO nanosheets (**b**) and the schematic diagrams of photocatalysis for NO sensing (**c**) [51]

of ZnO@Pt nanoflowers was developed for ethyl violet decomposition by Yuan et al. [36].

4.3 Other redox reactions

There have been few other applications for redox reactions of small molecules using noble metal–ZnO nanocompostes. The CO oxidation was studied as a potential application of Pt–ZnO nanocomposites by Burton et al. [22]. Prepared by an electrical method, the Pt–ZnO nanorods were used in the photoelectrochemical water splitting with a good performance [33].

5 Challenges and perspectives on future research

Since the synthesis methods, structures and applications of noble metal–ZnO nanocomposites have already been largely researched, few improvements of the material property can be further developed by adjusting the operating conditions or changing the nano-shapes. Thus, based on the above works, recently many other nanostructures have been explored by modification with different materials for enhanced or specific applications. The metal ion doping has been used as a method to further improve the catalytic activity of noble metal–ZnO nanostructures. Peng et al. [56] used Mg^{2+} doping to modify the Pd–ZnO nanostructure (Fig. 8a) for an enhanced oxidative coupling of carbon monoxide to dimethyl oxalate (Fig. 8b, c). The Pd/Mg–ZnO was produced by mixing molecules in solution and calcining them at high temperature for hours. Unlike the Mg^{2+} doping, graphene as a widely researched nanomaterial was also used with noble metals and ZnO to produce the multi-hybrid nanostructures [8]. The, Pd-, Ag-, Pt- and Au-graphene–ZnO nanostructures were fabricated through two steps: mixing graphene with ZnO nanorods in solution and heating the sample in autoclave at 180 °C for 3 h to produce graphene–ZnO nanocomposites; loading Pd, Ag, Pt or Au nanoparticles on the graphene–ZnO nanocomposites with UV-irradiation for 30 min. The noble metal-graphene–ZnO nanostructures were found to have high electrocatalysis for H_2O_2 reduction, with the decreasing order of electrocatalytic activity: Pd-graphene–ZnO > Ag-graphene–ZnO > Pt-graphene–ZnO > Pt-graphene–ZnO. The nanoparticle size of noble metal, distribution of nanoparticles and nanostructures were believed to have important impacts as the species of noble metal on their electrocatalytic activity. Another work using graphene as a part of Pt- and Pd–ZnO nanocomposites was reported by Li et al. [57], using a similar approach (mixing and annealing). The graphene enhanced noble metal–ZnO nanocomposites showed a high methanol oxidation under visible-light exciting. Apart from graphene (C)-doping, Patil et al. [69] enhanced the photocatalytic activity of zinc oxide by

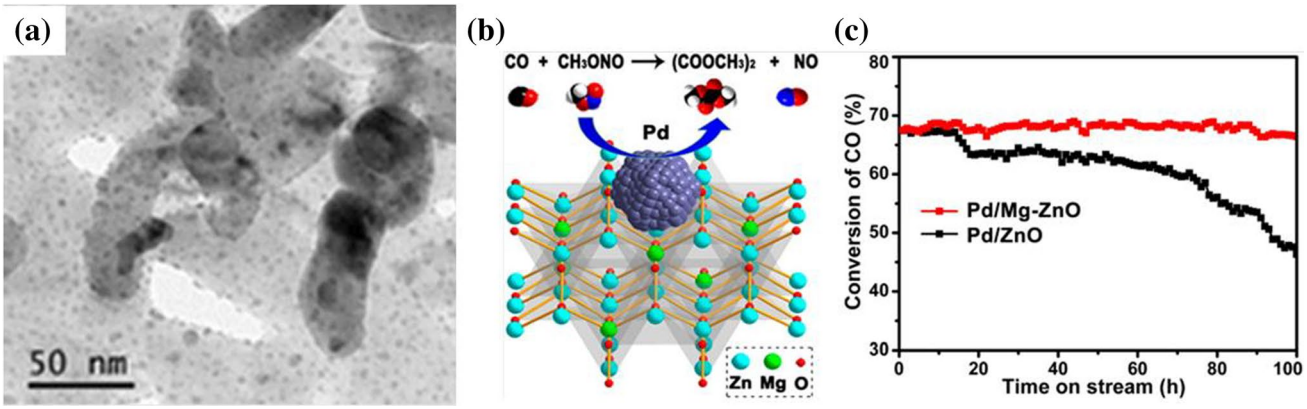

Fig. 8 The TEM image of Mg^{2+}-doped Pd–ZnO nanostructure (**a**) and the enhanced oxidative coupling of carbon monoxide to dimethyl oxalate (**b, c**) [56]

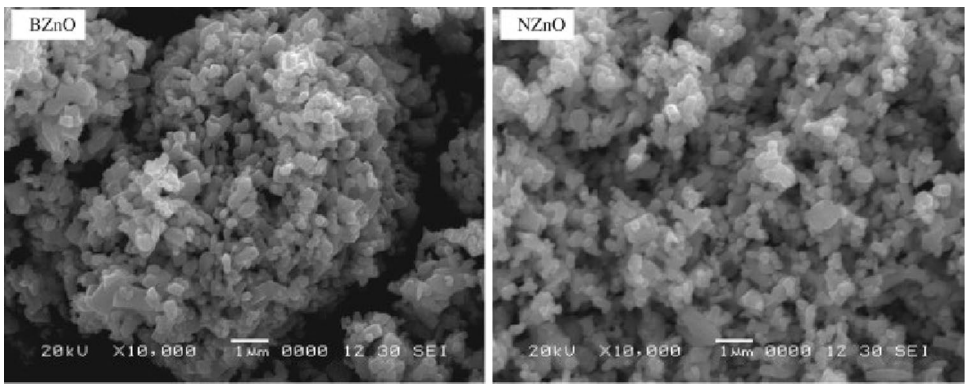

Fig. 9 SEM images of B-doped ZnO and N-doped ZnO [69]

incorporation of nonmetal (B- and N-doped ZnO, SEM images shown in Fig. 9). Although the enhancement of photocatalytic activity by incorporation of nonmetal might be not as efficient as metals, the ability of photocatalytic degradation for their as-prepared materials was in the order of: BZnO > NZnO > ZnO.

On the other hand, future studies should also focus on the applications using the synthesized materials. In general, the photoluminescence lifetime is an important parameter for their applications. The lifetime of ZnO nanostructures has been found to reply on the size [70] and structure [71]. For instance, the lifetime is about 1 ns for ZnO single crystals [9]. ZnO epilayers have the lifetime of 2.5–3.8 ns [72, 73]. The combination of noble metal reduces the excitons lifetime of ZnO, leading to quicker energy transfer between the ZnO and noble metal [74, 75]. As shown in Fig. 10 [76], the lifetimes of pure ZnO, 2 mL-Ag/ZnO and 8 mL-Ag/ZnO are 1.57, 1.02 ns and 1.05, respectively, showing that the lifetime of noble metal–ZnO nanocomposites replies on the noble metal concentration. Therefore design, synthesis and optimization of the noble metal–ZnO nanocomposites would be the future works for scientists and engineers in this field.

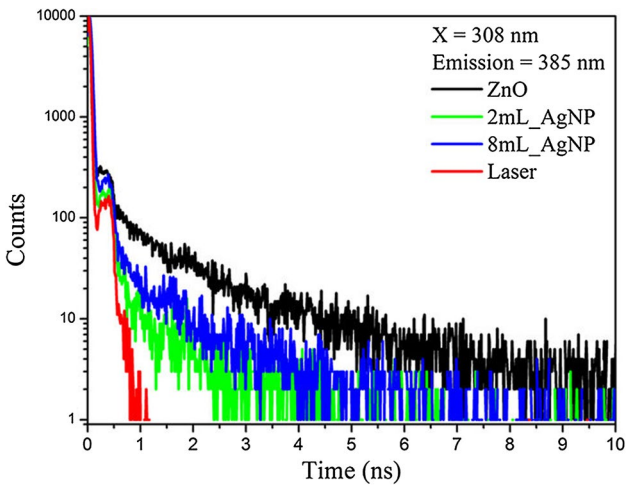

Fig. 10 The decreased lifetime for the samples containing silver nanoparticles is attributed to plasmon-coupled emission mechanism [76]

6 Conclusions

To date, the numbers of the published papers about each of the noble metal–ZnO nanocomposites are 175,000

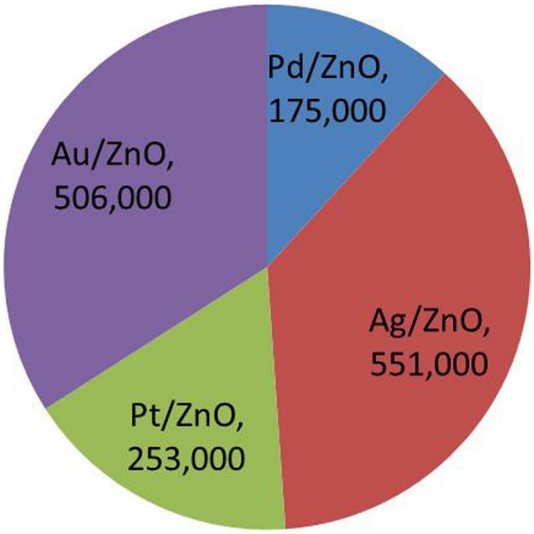

Fig. 11 The number of the published papers about each of the noble metal–ZnO nanocomposites

(Pd–ZnO), 551,000 (Ag–ZnO), 253,000 (Pt–ZnO) and 506,000 (Au–ZnO), respectively (Fig. 11). Noble metal–ZnO nanocomposites have been considered one of the most practical photo-catalyst, gaining increasing interest due its high catalytic property, and super stability. In this review, the noble metal–ZnO nanocomposites with various composites and structures for catalytic applications will be discussed. We introduce the multi-catalytic properties and design concept of the noble metal–ZnO nanocomposites, and then particular highlight key finding of synthesis method for various noble metal–ZnO nanocomposites. The catalytic activity of noble metal–ZnO nanostructures has been found to rely on not only the species of noble metal but also the architecture of the catalyst material. Moreover, the typical works of modification on noble metal–ZnO nanostructures have been introduced. Critically, the challenges for future research development and our future perspectives are presented.

Acknowledgements This work has been financially supported by National Natural Science Foundations of China (51202197 and 51372205) and the National "973" Program (2011CB610406). It is also supported by the Specialized Research Fund for the Doctoral Program of Higher Education of China (20116102120014), and the Natural Science Basic Research Plan in Shaanxi Province of China (2014K06-13).

References

1. T.T. Zhuang, Y. Liu, Y. Li et al., Small **13**, 1602629 (2017)
2. J. Gan, X. Lu, Y. Tong, Nanoscale **6**, 7142 (2014)
3. G.-L. Wang, K.-L. Liu, Y.-M. Dong, X.-M. Wu, Z.-J. Li, C. Zhang, Biosens. Bioelectron. **62**, 66 (2014)
4. X. Lang, J. Zhao, X. Chen, Chem. Soc. Rev. **45**, 3026 (2016)
5. M.D. Regulacio, M.-Y. Han, Acc. Chem. Res. **49**, 511 (2016)
6. C.-C. Wang, X.-D. Du, J. Li, X.-X. Guo, P. Wang, J. Zhang, Appl. Catal. B **193**, 198 (2016)
7. T. Yanagitani, N. Mishima, M. Matsukawa, Y. Watanabe, IEEE Trans. Ultrason. Ferroelectr. Freq. Control **54**, 701 (2007)
8. H Gu, Y Yang, J Tian, G Shi, Acs Appl. Mater. Interfaces **5**, 6762 (2013)
9. Ü Özgür, Y.I. Alivov, C. Liu et al., J. Appl. Phys. **98**, 11 (2005)
10. X. Sun, S. Lam, T. Sham, F. Heigl, A. Jürgensen, N. Wong, J. Phys. Chem. B **109**, 3120 (2005)
11. A. Kołodziejczak-Radzimska, T. Jesionowski, Materials **7**, 2833 (2014)
12. C. Yu, K. Yang, Y. Xie et al., Nanoscale **5**, 2142 (2013)
13. H. Liu, Y. Feng, D. Chen, C.Y. Li, P.L. Cui, J. Yang, J. Mater. Chem. A **3**, 3182 (2015)
14. M. Pirhashemi, A. Habibi-Yangjeh, J. Colloid Interface Sci. **491**, 216 (2017)
15. B. Golzad-Nonakaran, A. Habibi-Yangjeh, Mater. Chem. Phys. **184**, 210 (2016)
16. B. Golzad-Nonakaran, A. Habibi-Yangjeh, Adv. Powder Technol. **27**, 1427 (2016)
17. M. Pirhashemi, A. Habibi-Yangjeh, J. Mater. Sci. **27**, 4098 (2016)
18. M. Pirhashemi, A. Habibi-Yangjeh, J. Alloys Compd. **601**, 1 (2014)
19. S. Shaker-Agjekandy, A. Habibi-Yangjeh, Mater. Sci. Semicond. Process **34**, 74 (2015)
20. S. Naghizadeh-Alamdari, A. Habibi-Yangjeh, M. Pirhashemi, Solid State Sci. **40**, 111 (2015)
21. J. Chiou, S. Ray, H. Tsai et al., J. Phys. Chem. C **115**, 2650 (2011)
22. P.D. Burton, D. Lavenson, M. Johnson et al., Top. Catal. **49**, 227 (2008)
23. D. Zhang, X. Liu, X. Wang, J. Alloys Compd. **509**, 4972 (2011)
24. J. Liqiang, W. Baiqi, X. Baifu et al., J. Solid State Chem. **177**, 4221 (2004)
25. T.-J. Whang, M.-T. Hsieh, H.-H. Chen, Appl. Surf. Sci. **258**, 2796 (2012)
26. B. Baruwati, D.K. Kumar, S.V. Manorama, Sens. Actuators B **119**, 676 (2006)
27. S.M. Majhi, P. Rai, Y.-T. Yu, Acs Appl. Mater. Interfaces **7**, 9462 (2015)
28. C.S. Rout, A. Raju, A. Govindaraj, C. Rao, Solid State Commun. **138**, 136 (2006)
29. N. Morales-Flores, U. Pal, E.S. Mora, Appl. Catal. A **394**, 269 (2011)
30. C. Liewhiran, S. Phanichphant, Curr. Appl. Phys. **8**, 336 (2008)
31. P. Pawinrat, O. Mekasuwandumrong, J. Panpranot, Catal. Commun. **10**, 1380 (2009)
32. Y. Chen, D. Zeng, K. Zhang, A. Lu, L. Wang, D.-L. Peng, Nanoscale **6**, 874 (2014)
33. Y.K. Hsu, S.Y. Fu, M.H. Chen, Y.C. Chen, Y.G. Lin, Electrochim. Acta **120**, 1 (2014)
34. D.-T. Phan, G.-S. Chung, Sens. Actuators B **161**, 341 (2012)
35. S. Wei, Y. Yu, M. Zhou, Mater. Lett. **64**, 2284 (2010)
36. J. Yuan, E.S.G. Choo, X. Tang, Y. Sheng, J. Ding, J. Xue, Nanotechnology **21**, 185606 (2010)
37. J. Liqiang, W. Dejun, W. Baiqi, et al, J. Mol. Catal. A **244**, 193 (2006)
38. Y. Zhang, Q. Xiang, J. Xu, P. Xu, Q. Pan, F. Li, J. Mater. Chem. **19**, 4701 (2009)
39. A. Bera, D. Basak, Nanotechnology **22**, 265501 (2011)
40. C.-M. Chang, M.-H. Hon, C. Leu, Rsc Adv. **2**, 2469 (2012)
41. Y. Xiao, L. Lu, A. Zhang et al., Acs Appl. Mater. Interfaces **4**, 3797 (2012)

42. P. Bera, J.M. Vohs, J. Phys. Chem. C **111**, 7049 (2007)
43. L.-L. Xing, C.-H. Ma, Z.-H. Chen, Y.-J. Chen, X.-Y. Xue, Nanotechnology **22**, 215501 (2011)
44. C. Yu, K. Yang, W. Zhou, Q. Fan, L. Wei, C.Y. Jimmy, J. Phys. Chem. Solids **74**, 1714 (2013)
45. D. Lin, H. Wu, W. Zhang, H. Li, W. Pan, Appl. Phys. Lett. **94**, 172103 (2009)
46. H. Li, E.-T. Liu, F.Y. Chan, Z. Lu, R. Chen, Mater. Lett. **65**, 3440 (2011)
47. X.-Y. Ye, Y.-M. Zhou, Y.-Q. Sun, J. Chen, Z.-Q. Wang, J. Nanopart. Res. **11**, 1159 (2009)
48. W. Lu, S. Gao, J. Wang, J. Phys. Chem. C **112**, 16792 (2008)
49. X.-Y. Xue, Z.-H. Chen, L.-L. Xing, C.-H. Ma, Y.-J. Chen, T.-H. Wang, J. Phys. Chem. C **114**, 18607 (2010)
50. L. He, L. Li, T. Wang et al., Dalton Trans. **43**, 16981 (2014)
51. N. Gogurla, A.K. Sinha, S. Santra, S. Manna, S.K. Ray, Sci. Rep. **4**, 6483 (2014)
52. P. Li, Z. Wei, T. Wu, Q. Peng, Y. Li, J. Am. Chem. Soc. **133**, 5660 (2011)
53. X-j Wang, W. Wang, Y.-L. Liu, Sens. Actuators B **168**, 39 (2012)
54. L. Shen, N. Bao, K. Yanagisawa et al., J. Solid State Chem. **180**, 213 (2007)
55. L. Shen, N. Bao, K. Yanagisawa, A. Gupta, K. Domen, C.A. Grimes, Cryst. Growth Des. **7**, 2742 (2007)
56. S.-Y. Peng, Z.-N. Xu, Q.-S. Chen et al., ACS Catal. **5**, 4410 (2015)
57. Z. Li, L. Ye, F. Lei, Y. Wang, S. Xu, S. Lin, Electrochim. Acta **188**, 450 (2016)
58. S. Choopun, A. Tubtimtae, T. Santhaveesuk, S. Nilphai, E. Wongrat, N. Hongsith, Appl. Surf. Sci. **256**, 998 (2009)
59. N. Bala, S. Saha, M. Chakraborty et al., Rsc Adv **5**, 4993 (2015)
60. A. Mclaren, T. Valdes-Solis, G. Li, S.C. Tsang, J. Am. Chem. Soc. **131**, 12540 (2009)
61. B.I. Kharisov, Recent Pat. Nanotechnol. **2**, 190 (2008)
62. S. Tan, A. Ebrahimi, T. Langrish, Mater. Des. **117**, 178 (2017)
63. H. Huang, N. Huang, Z. Wang et al., J. Colloid Interface Sci. **502**, 77 (2017)
64. A. Blaková, L. Csölleová, V. Brezová, J. Photochem. Photobiol. A **113**, 251 (1998)
65. W. Göpel, G. Rocker, R. Feierabend, Phys. Rev. B **28**, 3427 (1983)
66. X. Liu, H. Cao, J. Yin, Nano Res. **4**, 470 (2011)
67. Z. Bao, Y. Yuan, C. Leng, L. Li, K. Zhao, Z. Sun, Acs Appl. Mater. Interfaces **9**, 16417 (2017)
68. M.R.D. Khaki, M.S. Shafeeyan, A.A.A. Raman, W.M.A.W. Daud, J. Environ. Manage. **198**, 78 (2017)
69. A.B. Patil, K.R. Patil, S.K. Pardeshi, J. Solid State Chem. **184**, 3273 (2011)
70. G. Xiong, U. Pal, J.G. Serrano, J. Appl. Phys. **101**, 024317 (2007)
71. W. Kwok, A. Djurišić, Y. Leung, W. Chan, D. Phillips, Appl. Phys. Lett. **87**, 223111 (2005)
72. A. Tsukazaki, A. Ohtomo, T. Onuma et al., Nat. Mater. **4**, 42 (2005)
73. S. Chichibu, T. Onuma, M. Kubota et al., J. Appl. Phys. **99**, 093505 (2006)
74. J.R. Lakowicz, Anal. Biochem. **337**, 171 (2005)
75. Q. Ren, S. Filippov, S. Chen et al., Nanotechnology **23**, 425201 (2012)
76. E. Guidelli, O. Baffa, D. Clarke, Sci. Rep. **5**, 14004 (2015)